J Appl Electrochem (2012) 42:271–277
DOI 10.1007/s10800-012-0397-1

ORIGINAL PAPER

A hydroxylamine electrochemical sensor based on electrodeposition of platinum nanoclusters on choline film modified glassy carbon electrode

Jing Li · Huaqing Xie

Received: 29 November 2011 / Accepted: 18 February 2012 / Published online: 2 March 2012

Abstract A sensitive hydroxylamine sensor was developed based on electrodeposition of Pt nanoclusters on choline film modified glassy carbon electrode (nano-Pt/Ch/GCE). The properties of the composites were characterized by field emission scanning electron microscope, X-ray photoelectron spectroscopy, powder X-ray diffraction, and electrochemical investigations. The designed nano-Pt/Ch/GCE showed a high sensing performance for hydroxylamine in a wide concentration ranges of 5.0×10^{-7}–1.1×10^{-3} M and 1.1×10^{-3}–19×10^{-3} M. The detection limit was 0.07 μM ($s/n = 3$). The proposed electrode presented excellent operational and storage stability for the determination of hydroxylamine. Moreover, the sensor showed good sensitivity, selectivity, and reproducibility properties. All the results indicated the designed sensor had a good potential application in the determination of hydroxylamine.

Keywords Electrocatalytic oxidation · Choline · Pt nanoclusters · Hydroxylamine

1 Introduction

Hydroxylamine is widely used as a kind of reducing agents and raw materials in industry and pharmacy [1]. It is identified as one of the intermediate products in many biological processes [2]. Hydroxylamine is also a well-known mutagen, moderately toxic to humans, animals, and plants [3]. Thus, it is important to develop sensitive analytical methods for quantitative determination of hydroxylamine [4]. Recently, numerous methods have been developed to determine hydroxylamine, such as ion chromatography [1], spectrophotometry [5, 6], gas chromatography [7], biamperometry [8], and capillary electrophoresis [9]. However, the processes involved in these methods are extremely complex, and the linear ranges are relatively narrow. Electroanalytical technique is a simple and effective method for the determination of hydroxylamine. Moreover, the investigation of hydroxylamine electrochemical reactivity is important from a fundamental point of view. However, hydroxylamine exhibits irreversible oxidation requiring large overpotential at conventional electrodes. Recently, various chemically modified electrodes (CMEs) have been constructed and applied in the determination of hydroxylamine [10–16], which can significantly lower the overpotential and enhance the oxidation current response.

Noble metal nanomaterials have been extensively investigated in recent years, owing to their unique optical, electrochemical, and electronic performances [17–22]. Metal nanoparticles can cause enhancement of effective surface area and accelerate the electron exchange rate between the electrode and the analyte. In particular, Pt nanoparticles have been used increasingly in many electrochemical applications, due to its role in enhancing the electrode conductivity and facilitating the electron transfer rate [23–27].

In this study, a new hydroxylamine sensor is constructed based on the electrodeposition of Pt nanoclusters on choline film modified glassy carbon electrode. As a precursor of acetylcholine, choline plays an important role in maintaining the central nervous system and numerous metabolic functions [28]. Choline can be also grafted onto the carbon electrode through nucleophilic attack reaction between oxidized carbon and the –OH group [29]. The positively

J. Li · H. Xie (✉)
School of Urban Development and Environmental Engineering, Shanghai Second Polytechnic University, Shanghai 201209, People's Republic of China
e-mail: hqxie@eed.sspu.cn

charged choline film could facilitate the formation of Pt nanoclusters through the electrostatic interaction between $-N^+(CH_3)_3$ polar head group and $PtCl_6^{2-}$. The fabricated nano-Pt/Ch composites films exhibited high stability and excellent catalytic activity toward hydroxylamine oxidation, which can be used as an effective hydroxylamine electrochemical sensor.

2 Experimental

2.1 Reagents

Hydroxylamine, choline, $LiClO_4$, and K_2PtCl_6 were purchased from Chemical Reagent Company of Shanghai (Shanghai, China). All other chemicals were analytical reagent grade and used without further purification. The 0.1 M phosphate buffer solutions (PBSs) of different pH values were prepared for the study. All electrochemical experiments were carried out at ambient temperature.

2.2 Apparatus

All electrochemical measurements were performed on electrochemical workstation CHI 660C (ChenHua Instruments Co., Shanghai, China). A conventional three-electrode system was used. A glassy carbon electrode (GCE, $\Phi = 4.0$ mm) served as the basal working electrode. A platinum wire and a saturated calomel electrode (SCE) were used as the counter electrode and the reference electrode, respectively. Electrochemical impedance spectroscopy (EIS) was investigated in 10 mM $K_3[Fe(CN)_6]$/$K_4[Fe(CN)_6]$ (1:1 mixture) solution containing 0.1 mol l^{-1} KCl in an electrochemical cell.

The images of the electrode surfaces were conducted on S-4800 field emission scanning electron microanalyser (Hitachi, Japan). X-ray photoelectron spectroscopy (XPS) measurements were performed on ESCALAB MK2 spectrometer (VG Co., UK). XRD measurements were recorded on X-ray diffraction system (D8-Advance, Germany) equipped with Cu K_α radiation ($\lambda = 1.54056$ Å).

2.3 Electrode preparation

Prior to modification, the basal GCE was polished with emery papers and slurries of alumina polishing powder to a mirror finish. After each polishing, the electrode was treated in ethanol and water in an ultrasonic bath for 5 min, respectively. Finally, it was dried under N_2 atmosphere ready for use.

The choline film was electrodeposited on the GCE by cyclic voltammetry (CVs) in 1 mM choline solution containing 10 mM $LiClO_4$ with a potential scanning from -1.7 to 1.8 V at a scan rate of 20 mV s^{-1} for 6 cycles. Then, the electrode was rinsed with water and sonication for 10 min to remove any physically adsorbed substance. The choline film has been strongly grafted onto the GCE surface through covalent bond, not simply attached to the electrode surface by physical adsorption. The choline modified electrode was obtained and denoted as Ch/GCE. The Pt nanoclusters was electrodeposited on the Ch/GCE under CV scanning from 0.4 to -0.2 V in 0.5 M H_2SO_4 solution containing 2 mM K_2PtCl_6 at a scan rate of 50 mV s^{-1} for 15 cycles. Then the modified electrode was taken out and rinsed with water, denoted as nano-Pt/Ch/GCE. For a comparison, the same Pt deposition process was conducted at bare GCE and denoted as nano-Pt/GCE.

3 Results and discussion

3.1 Characterization of the modified electrode surface

The morphology of the electrode surface was characterized by FE-SEM. Figure 1a showed the image of Pt nanoclusters on bare GCE (nano-Pt/GCE). It can be seen that the diameter of Pt is about 100–130 nm. Figure 1b illustrated the morphology of nano-Pt/Ch composites on the GCE. From the image, it can be observed that the Pt nanoclusters are homogeneously distributed on the choline film with diameter of 60–100 nm. The diameter is smaller than that observed on the nano-Pt/GCE. From the image, it can be also seen that the larger Pt is comprised of much smaller Pt nanoparticles.

The nano-Pt/Ch composites were further investigated by XPS determination. As shown in Fig. 2a, the Pt 4f spectrum consisting of two peaks located at 71.0 and 74.4 eV, corresponding to the Pt $4f_{7/2}$ and $4f_{5/2}$ components, respectively. This is consistent with the Pt (0) formation. The powder XRD determination was also used to characterize the crystal structure of Pt nanoclusters. As seen in Fig. 2b, five bands appeared at 39.8°, 46.2°, 67.6°, 81.5°, and 86.1°, which were assigned to the diffractions of the (111), (200), (220), (311), and (222) planes of the face-centered cubic metal Pt structure, illustrating Pt have been successfully deposited onto the choline film. Based on the reflection peak at $2\theta = 39.8°$, an averaged diameter of the Pt particles was calculated to be 8 nm [30]. The results indicated the Pt of about 100 nm size were clusters of nanocrystallites of about 8 nm.

EIS is a powerful method to characterize the electrode properties. In the Nyquist plots, the semicircular portion of the impedance spectrum at high frequency represents the charge transfer-limited process, and the diameter of the semicircle equals to the surface charge transfer resistance (R_{ct}). The R_{ct} value depends on the dielectric and insulating

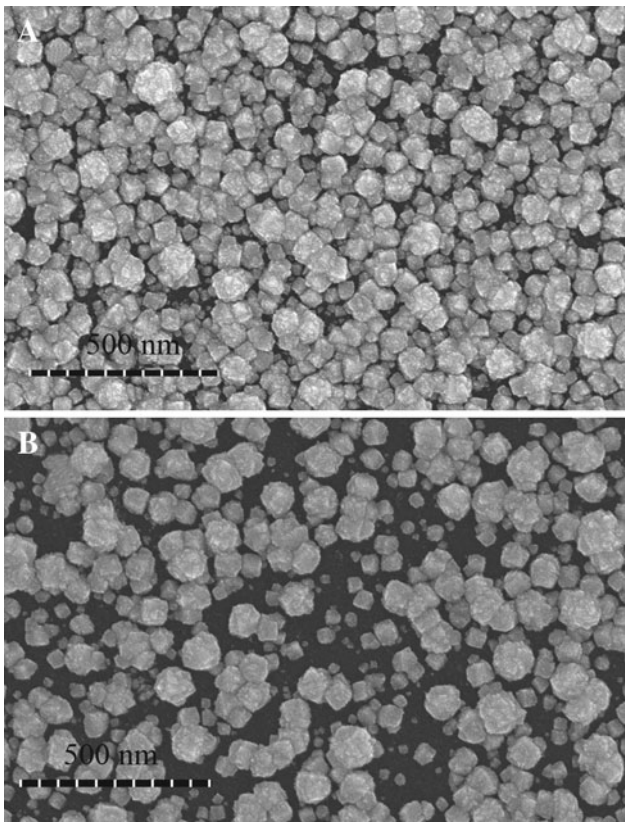

Fig. 1 FE-SEM images of nano-Pt/GCE (**a**) and nano-Pt/Ch/GCE (**b**)

properties of the electrode/electrolyte solution interface. Figure 3 showed the EIS of bare GCE, Ch/GCE, nano-Pt/GCE, and nano-Pt/Ch/GCE in 10 mM $K_3[Fe(CN)_6]$/$K_4[Fe(CN)_6]$ (1:1 mixture) solution containing 0.1 M KCl. The R_{ct} value of bare GCE (curve a) was 800 Ω. The diameter of the high-frequency semicircle was apparently reduced on the Ch/GCE. The R_{ct} value was 400 Ω (curve b). The positively charged choline film was favorable for approaching ferricyanide anions to the electrode surface. The R_{ct} value decreased to 300 Ω at the nano-Pt/GCE (curve c) and 200 Ω at the nano-Pt/Ch/GCE (curve d), respectively. These facts suggested that the electron transfer between $Fe(CN)_6^{3-/4-}$ electrochemical probe and the electrode was faster on the nano-Pt/Ch/GCE. The different R_{ct} value of the modification process indicated choline and Pt nanoclusters have been successfully immobilized on the GCE.

3.2 Electrocatalytic oxidation of hydroxylamine

In order to investigate the electrocatalytic behavior of nano-Pt/Ch/GCE towards hydroxylamine oxidation, CVs were obtained in comparison with bare GCE, Ch/GCE and nano-Pt/GCE in 6.0 × 10^{-4} M hydroxylamine solution. As shown in Fig. 4, there was no anodic peak current at the bare GCE (curve a). Ch/GCE made the current response larger than that

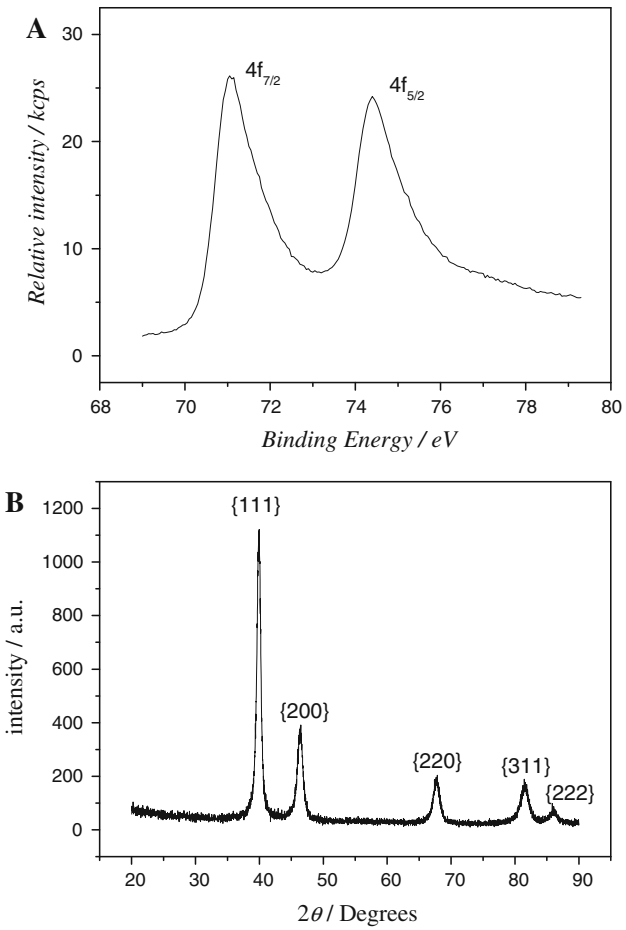

Fig. 2 XPS curve (**a**) and XRD pattern (**b**) of nano-Pt/Ch composites

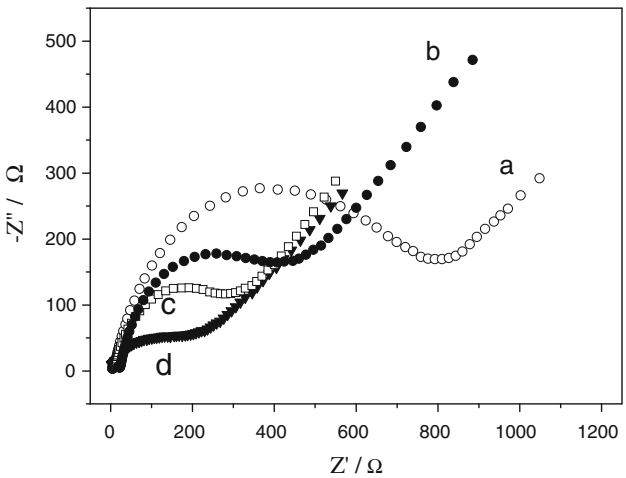

Fig. 3 EIS of bare GCE (*a*), Ch/GCE (*b*), nano-Pt/GCE (*c*) and nano-Pt/Ch/GCE (*d*) in 10.0 mM $K_3[Fe(CN)_6]$/$K_4[Fe(CN)_6]$ (1:1 mixture) + 0.1 M KCl

at the bare GCE (curve b). There was a dramatic enhancement of the peak current on the nano-Pt/GCE (curve c) relative to the Ch/GCE and the bare GCE. CVs of

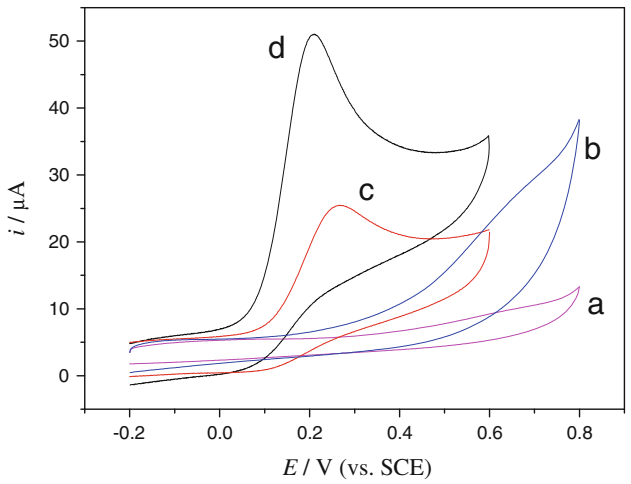

Fig. 4 CVs of 6.0×10^{-4} M hydroxylamine in 0.1 M PBS (pH 7.0) at bare GCE (*curve a*), Ch/GCE (*curve b*), nano-Pt/GCE (*curve c*), and nano-Pt/Ch/GCE (*curve d*). Scan rate: 50 mV s^{-1}

hydroxylamine on nano-Pt/GCE showed an irreversible wave with peak potential at 0.27 V. The large decrease of oxidation overpotential can be ascribed to the high density arrays of nano-Pt, which can improve reversibility of the electron transfer process. Furthermore, the nano-Pt/Ch/GCE showed a well-defined sharp catalytic oxidation peak towards hydroxylamine oxidation (curve d) and presented the peak potential at 0.21 V. The oxidation peak is shifted to 60 mV less positive potential and the peak current is 2 times higher in comparison with nano-Pt/GCE, reflecting the nano-Pt/Ch/GCE has a superior electrochemical performance. The comparisons revealed that the Pt nanoclusters have much stronger catalytic activity toward the oxidation of hydroxylamine than choline film, and the choline supported Pt nanoclusters have further enhanced catalytic activity. The increase of current response can be partly attributed to the high specific surface area and the increase of reversibility of the electron transfer process. The choline monolayer can effectively transfer electrons between the GCE and Pt active sites in hydroxylamine oxidation process. On the other hand, the choline film has a surface accumulation toward the electro-active species. The film can also reduce the amount of oxidation products accumulated to the catalytic sites, preventing the electrode from fouling. Furthermore, the supporting choline film can finely disperse the Pt nanoclusters and reduce the congregating tendency. The strategy of the combination of choline film and Pt nanoclusters exhibited significant advantages of synergic effect for construction of hydroxylamine electrochemical sensor.

The influence of scan rates on peak currents at the nano-Pt/Ch/GCE was investigated. The peak currents varied linearly with the scan rates from 10 to 300 mV s^{-1}, indicating an adsorption-controlled process. As faster electron transfer leads to a sharper and more well-defined peak, hydroxylamine can be effectively determined on the nano-Pt/Ch/GCE.

3.3 Effect of cycle number

Since Pt nanoclusters play an important role in the performance of electrochemical sensors, the influence of the amount of dispersed Pt onto the choline film is investigated by controlling the cycles of CV scanning. As shown in Fig. 5, when the cycle numbers increased, the response currents of hydroxylamine increased at first 15 cycles and then decreased. With CV cycles increased up to 15 cycles, larger Pt nanoclusters and higher coverage onto the choline film were observed. The enhanced surface area from the modification of Pt nanoclusters enables more available active sites on the electrode surface for hydroxylamine oxidation. While the cycle numbers are further increased, the Pt would be continuously generated, even significant aggregated, resulting in decreasing sensing performance. Thus, the condition of 15 potential cycles is optimal for the preparation of nano-Pt/Ch composites modified GCE.

3.4 Effect of solution pH

The oxidation of hydroxylamine showed a strong dependence on pH, so pH should be optimized for its determination. As shown in Fig. 6, the oxidation current increased remarkably with increasing pH from 4 to 7 and then increased indistinctively between 7 and 10. Hydroxylamine presents two forms in solutions, including the non-protonated form of NH_2OH for pH higher than 5.9 and protonated form of NH_3OH^+ at lower pH than 5.9 ($pK_a = 5.9$). The protonated NH_3OH^+ is less active in comparison with non-protonated form in the oxidation process. It is also found that the peak potential shifts positively along with the decrease of

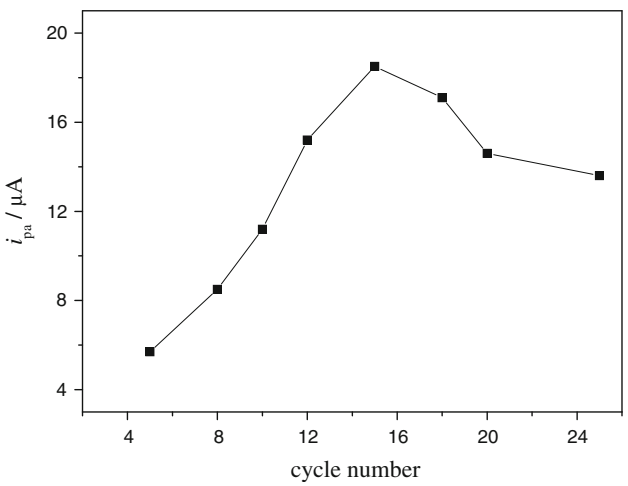

Fig. 5 Effects of potential scanning cycles in 2 mM K_2PtCl_6 + 0.5 M H_2SO_4. Hydroxylamine concentration: 2.5×10^{-4} M

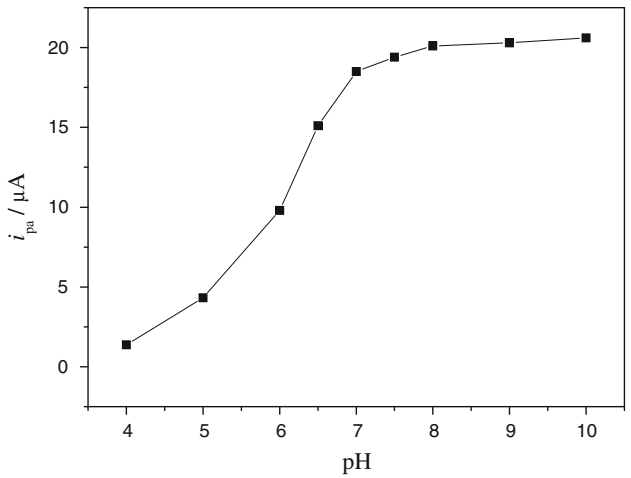

Fig. 6 Dependence of LSV anodic peak current at nano-Pt/Ch/GCE on the pH in 2.5×10^{-4} M hydroxylamine solutions. Scan rate: 50 mV s^{-1}

pH, indicating the overpotential of hydroxylamine oxidation in acid solution is large. Considering the practically applications, pH 7.0 PBS is chosen as the supporting electrolyte in our experiments.

3.5 Determination of hydroxylamine

Linear sweep voltammetry (LSV) techniques were used to determine hydroxylamine. Very well-defined voltammograms were obtained on the nano-Pt/Ch/GCE, as shown in Fig. 7A. The plot of the peak current (i_{pa}) versus hydroxylamine concentrations was shown in Fig. 7B. A good linearity consisted of two segments was obtained in the range of 5.0×10^{-7}–1.1×10^{-3} M with a current sensitivity of 64.8 μA mM^{-1}, and in the range of 1.1×10^{-3} – 19×10^{-3} M with a current sensitivity of 29.3 μA mM^{-1}. The calibration curve of two linear segments may be attributed to the generation of N_2O on the Pt catalytic sites and thus change the surface reaction conditions. At low hydroxylamine concentrations, there is little N_2O bubble throughout the electrode. The formed N_2O does not strongly adsorb on Pt surface. It could quickly dissolve into the solution and may not influence the hydroxylamine oxidation process. At high concentrations, the N_2O may form bubbles adhesive at the catalytic sites and inhibit the oxidation of new hydroxylamine molecules, result in uncertainty of current response. However, the N_2O bubble has not been observed in our experiments. The current response is reproducible with a relative standard deviation (RSD) of 2.5% for 15 repetitive determinations. The linear response obtained at low concentrations can be used to construct a hydroxylamine sensor. According to the former calibration plot, the detection limit was found to be 0.07 μM ($s/n = 3$).

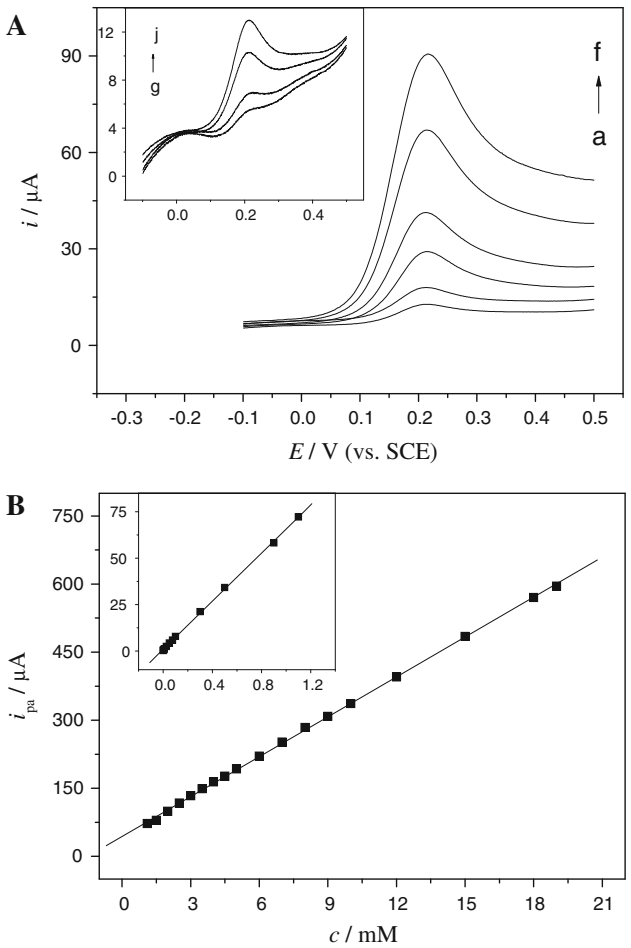

Fig. 7 **A** LSVs of different concentrations of hydroxylamine at nano-Pt/Ch/GCE (*a–f*): 7.5×10^{-5}, 1.0×10^{-4}, 3.0×10^{-4}, 5.0×10^{-4}, 9.0×10^{-4}, 1.1×10^{-3} M. *Inset* presents LSVs of low concentrations of hydroxylamine (*g–j*): 5.0×10^{-7}, 5.0×10^{-6}, 2.5×10^{-5}, 5.0×10^{-5} M. Scan rate: 50 mV s^{-1}. **B** The corresponding calibration curves for hydroxylamine

The dynamic range, current sensitivity and the detection limit of nano-Pt/Ch/GCE for the determination of hydroxylamine were compared with the reported CMEs. As shown in Table 1, the designed nano-Pt/Ch/GCE exhibited relatively low detection limit, high current sensitivity and two wide linear regions. The advantages of the nano-Pt/Ch/GCE can be attributed to the composite structure formed by the choline layer and well-dispersed Pt nanoclusters, which have synergic effect of organic and metallic nanoclusters toward hydroxylamine oxidation.

3.6 Interference test

An important problem in determining hydroxylamine is the presence of other nitrogen containing compounds, such as nitrate, nitrite, ammonia, and hydrazine, which often accompany with hydroxylamine in various industrial and

Table 1 Comparisons of the responses of some hydroxylamine sensors constructed based on different modified electrodes

Electrode	Detection limit (μM)	Sensitivity (μA mM^{-1})	Linear range (μM)	References
APS/GCE[a]	7.2	73.9	10–800	[11]
RMWCNT/GCE	1	28.8	1–33.8	[12]
		25	33.8–81.7	
ZnO/MWCNTs/GCE	0.12	7.45	0.4–19,000	[14]
NiCoHCF/GCE	0.23	4.94	20–200	[15]
			200–10,000	
Au/PPy/GCE	0.21	63.9	1–500	[16]
		10.4	500–18,000	
nano-Pt/Ch/GCE	0.07	64.8	0.5–1,100	This work
		29.3	1,100–19,000	

RMWCNT/GCE rutin multi-wall carbon nanotubes modified glassy carbon electrode, *ZnO/MWCNTs/GCE* ZnO nanofilms attached multi-walled carbon nanotubes (MWCNTs) modified glassy carbon electrodes, *NiCoHCF/GCE* hybrid nickel–cobalt hexacyanoferrate film modified glassy carbon electrode, *Au/PPy/GCE* gold nanoparticle-polypyrrole nanowire modified glassy carbon electrode

[a] Alizarine red S (ARS) as a homogenous mediator

biological processes. The tolerance limit of potentially interfering substances is defined as the molar ratio of the additive/hydroxylamine causing relative error <5%. The results showed that 350-fold NO_3^-, NO_2^-, 10-fold NH_3^+, and 1-fold hydrazine have no interference on 1.0×10^{-5} M hydroxylamine determination. The interfering effect of other common ions has also investigated. The results showed that 380-fold Cl^-, Br^-, F^-, I^-, HCO_3^-, PO_4^{3-}, CO_3^{2-}, $C_2O_4^{2-}$, SO_4^{2-}, Na^+, K^+, Mg^{2+}, Ca^{2+}, Ba^{2+}, Cu^{2+}, Ni^{2+}, Zn^{2+}, Fe^{3+}, Fe^{2+}, and Al^{3+}, 160-fold glucose, sucrose, fructose, oxalic acid, tartaric acid, citric acid, and malic acid, 25-fold L-tyrosine, L-arginine and L-glutamic acid, 20-fold peptide, and alpha-fetoprotein, did not interfere with the determination of hydroxylamine.

3.7 Application to sample analysis

The performance and validity of the nano-Pt/Ch/GCE in the analysis of hydroxylamine was investigated. Two water samples of the ground water and auxiliary cooling water from power generation management were used for measurement. 5 ml of fresh water samples were added into each of the series of 50-ml voltammetric flasks. The samples were analyzed without previous treatment for elimination of organic substances or other components. Different standard concentration of hydroxylamine were added to the flasks and made up to volume with the supporting electrolyte solution. 5 ml of this solution was placed into the electrochemical cell for analyzing under optimized conditions using the above technique. The results were listed in the Table 2. The results obtained by standard addition method showed satisfactory recovery, demonstrating the nano-Pt/Ch/GCE could be efficiently used for practical applications.

Table 2 Recovery of hydroxylamine from different water samples

Samples	Added (μM)	Found[a] (μM)	Recovery (%)	RSD (%)
Ground water	0	<Detection limit	–	–
	5.0	5.1 ± 0.1	102	2.4
	10.0	10.1 ± 0.3	101	2.2
	15.0	14.7 ± 0.3	98	2.3
	20.0	20.4 ± 0.2	102	2.1
Auxiliary	0	2.4 ± 0.2	–	3.3
Cooling water	5.0	7.5 ± 0.2	101	3.2
	10.0	12.3 ± 0.2	99	2.8
	15.0	17.8 ± 0.2	102	2.5
	20.0	22.6 ± 0.2	101	2.4

[a] Average of five determinations

3.8 Stability and reproducibility

The electrochemical stability of the prepared electrodes was evaluated by repeating the CV test between −0.2 and 0.5 V at a scan rate of 50 mV s^{-1}. After 200 CV scanning, the oxidation peak current decreased 12% for the nano-Pt/GCE in comparison with 4% for the nano-Pt/Ch/GCE, demonstrating the nano-Pt/Ch/GCE has a good electrochemical stability. The storage ability of the modified electrode was also investigated. The designed electrode was stored in 0.1 M PBS (pH 7.0) at 4 °C. It was found that the current response to hydroxylamine on the nano-Pt/Ch/GCE was no apparent decrease in the first 7 days by everyday use. Only 7 and 20% decrease was found after 30 and 60 days, respectively. In comparison with nano-Pt/Ch/GCE, the nano-Pt/GCE only retained 87 and 70% of the initial values after 30 and 60 days, respectively. The results demonstrate the nano-Pt/Ch/GCE has higher stability than nano-Pt/GCE.

In order to characterize the reproducibility of the designed electrode, a series of repetitive measurements were carried out in 1.0×10^{-5} M hydroxylamine solution. The RSD of 2.5% was observed for 15 determinations. Five pieces of nano-Pt/Ch/GCE were prepared and the RSD for the individual determination of 1.0×10^{-5} M hydroxylamine was 2.8%. These results indicated that the sensor has good reproducibility and long-term stability. The high stability of the modified electrode can be related

to the choline layer, which can stabilize the activity of Pt nanoclusters.

4 Conclusions

A hydroxylamine electrochemical sensor was developed based on the nano-Pt/Ch composites comprised of choline layer and Pt nanoclusters. The choline provided a supporting layer to immobilize Pt nanoclusters on the GCE surface. In comparison with nano-Pt/GCE, the nano-Pt/Ch/GCE has superior catalytic activity toward hydroxylamine oxidation, providing a wider linear range, lower detection limit, higher current sensitivity, better reproducibility, and storage stability. The excellent catalytic ability of the designed sensor can be attributed to the synergic effect of the choline film and Pt nanoclusters. The strategy of the combination of choline film and Pt nanoclusters presents a significant advantage for construction of hydroxylamine sensor.

Acknowledgments This study was supported by the Shanghai Educational Development Foundation and the Shanghai Municipal Education Commission (11CG64), the Innovation Program of Shanghai Municipal Education Commission (12YZ179), the Program for New Century Excellent Talents in University (NCET-10-883), and the Program for Professor of Special Appointment (Eastern Scholar) at Shanghai Institutions of Higher Learning.

References

1. Fernando PN, Egwu IN, Hussain MS (2002) J Chromatogr A 956:261
2. Hofman T, Lees H (1953) Biochem J 54:579
3. Smith RP, Layne WR (1969) J Pharmacol Exp Ther 165:30
4. Kolasa T, Wardencki W (1974) Talanta 21:845
5. Veena K, Narayana B (2010) Oxid Commun 33:54
6. George M, Nagaraja KS, Balasubramanian N (2008) Chem Anal 53:315
7. Seike Y, Fukumori R, Senga Y, Oka H, Fujinaga K, Okumura M (2004) Anal Sci 20:139
8. Zhao C, Song JF (2001) Anal Chim Acta 434:261
9. Hu S, Zhang M, Pang DW, Cheng JK (2000) Anal Sci 16:807
10. Kannan P, John SA (2010) Anal Chim Acta 663:158
11. Ardakani MM, Karimi MA, Mirdehghan SM, Zare MM, Mazidi R (2008) Sens Actuators B 132:52
12. Zare HR, Sobhani Z, Mazloum-Ardakani M (2007) Sens Actuators B 126:641
13. Zare HR, Hashemi SH, Benvidi A (2010) Anal Chim Acta 668:182
14. Zhang CH, Wang GF, Liu M, Feng YH, Zhang ZD, Fang B (2010) Electrochim Acta 55:2835
15. Shi LH, Wu T, He P, Li D, Sun CY, Li JH (2005) Electroanalysis 17:2190
16. Li J, Lin XQ (2007) Sens Actuators B 126:527
17. Kokoh KB, Alonso-Vante N (2006) J Appl Electrochem 36:147
18. Cheng TT, Gyenge EL (2009) J Appl Electrochem 39:1925
19. Zhang JR, Chen Y, Li Y, Sun D, Tian DB, Zhu JJ (2011) J Mater Chem 21:7604
20. Li J, Lin XQ (2007) Anal Chim Acta 596:222
21. Upadhyay S, Rao GR, Sharma MK, Bhattacharya BK, Rao VK, Vijayaraghavan R (2009) Biosens Bioelectron 25:832
22. Weir MG, Knecht MR, Frenkel AI, Crooks RM (2010) Langmuir 26:1137
23. Ye F, Wang TT, Li JJ, Wang YL, Li JL, Wang XD (2009) J Electrochem Soc 156:B981
24. Wen ZH, Ci SQ, Li JH (2009) J Phys Chem C 113:13482
25. Raoof JB, Ojani R, Rashid-Nadimi S (2010) J Electroanal Chem 641:71
26. Li J, Lin XQ (2007) Biosens Bioelectron 22:2898
27. Li YJ, Gao W, Ci LJ, Wang CM, Ajayan PM (2010) Carbon 48:1124
28. Holm PI, Ueland PM, Kvalheim G, Lien EA (2003) Clin Chem 49:286
29. Jin GP, Lin XQ, Gong JM (2004) J Electroanal Chem 569:135
30. Radmilovic V, Gasteiger HA, Ross PN (1995) J Catal 154:98